

The Eurasia Proceedings of Science, Technology, Engineering and Mathematics (EPSTEM), 2025

Volume 38, Pages 807-815

**IConTES 2025: International Conference on Technology, Engineering and Science**

## **Effect of Variable Mass Density on Lengthwise Fracture in Functionally Graded Beams Moving in Horizontal Direction**

**Victor Rizov**

University of Architecture

**Abstract:** Functionally graded structural materials have been used with increasing intensity in various applications in different areas of up-to-date engineering during recent decades. This can be explained with excellent properties of these materials. Besides, the quickly developing technologies for producing different kinds of functionally graded materials also represent an important factor for increasing the application of these innovative materials. Using these materials for manufacturing moving components of various mechanisms and devices requires performing of analyses of the behavior of the components under inertia loadings. Developing fracture analysis under inertia loadings is very important in the context of safety and reliability. In view of this, the current paper is concerned with analyzing of a particular aspect of fracture, namely the effect of variable mass density on lengthwise fracture behavior of functionally graded beams moving in horizontal direction. The mass density varies along both thickness and length of the beam. The latter is under inertia loading due to beam acceleration in horizontal direction. The inertial loading of the beam is a continuous function of both thickness and length coordinates. The beam has non-linear viscoelastic behavior. The lengthwise fracture problem is treated by using the  $J$  integral method. A check-up is performed by analyzing the strain energy release rate. It is explored how the lengthwise fracture is influenced by the variable mass density and other parameters of the model.

**Keywords:** Variable mass density, Motion, Lengthwise fracture, Functionally graded beam

### **Introduction**

Functionally graded materials made by mixing of two or more constituents represent modern and highly efficient continuously inhomogeneous composites (Gandra et al., 2011; Mahamood & Akinlabi, 2017). One of the important advantages of functionally graded materials is that their properties change continuously in a solid. Besides, the change of their properties can be designed for achieving of certain goals (for instance, the goal can be strengthening of more heavily loaded parts of an engineering structure). With developing of the technologies for producing of these materials the area of their application quickly expands (Radhika et al., 2020; Shrikantha Rao & Gangadharan, 2014). The excellent properties of functionally graded materials allow construction of various structural members and components of different mechanisms and machines which in many cases are superior compared to those built-up by traditional homogeneous engineering materials (Fanani et al., 2021; Hedia et al., 2014; Wu et al., 2014).

The increasing use of functionally graded structural members and components in applications where they are involved in different mechanical motions requires performing detailed analyses of their fracture behavior under various inertia loadings. The practice indicates that fracture behavior is of primary importance for load-bearing capacity and safety of structures. Since functionally graded structures may be constructed layer-by-layer, they are prone to lengthwise fracture, i.e. appearance of lengthwise cracks (Dolgov, 2024; Mahamood & Akinlabi, 2017; Rizov & Altenbach, 2019; Rizov, 2024). In many situations these lengthwise cracks are the cause of structural failure under inertia loading. All this shows that studying of lengthwise fracture is representational

---

- This is an Open Access article distributed under the terms of the Creative Commons Attribution-Noncommercial 4.0 Unported License, permitting all non-commercial use, distribution, and reproduction in any medium, provided the original work is properly cited.

- Selection and peer-review under responsibility of the Organizing Committee of the Conference

© 2025 Published by ISRES Publishing: [www.isres.org](http://www.isres.org)

components subjected to different inertia loadings represents a problem of great meaning for both theoretical science and engineering practice.

In this context, the current paper is dealing with analysis of lengthwise fracture in a functionally graded beam structure that is moving in horizontal direction. The beam acted upon by inertial loading has non-linear viscoelastic behavior. One of the main purposes is to examine the effect of variable mass density on the lengthwise fracture (since the beam is functionally graded along thickness and length, the mass density varies continuously in both thickness and length directions). The lengthwise fracture is analyzed by the integral  $J$ . For this purpose, the acceleration induced inertia loading is determined and applied on the beam when solving the integral  $J$ . The viscoelastic behavior of the beam is treated by a non-linear modification of the Maxwell model. In this relation, the stress-strain-time law of the model under time-dependent stress is derived. A check-up of the integral  $J$  is performed by analyzing the strain energy release rate in the beam under inertia loading. The results obtained reveal how the lengthwise fracture is influenced by the variable mass density. The effect of variation of some other parameters along with the thickness and length of the beam on the lengthwise fracture is also studied.

### Theoretical Model

The functionally graded beam structure depicted in Figure 1 is analyzed in the current paper. The beam is moving in horizontal direction. The law of beam motion is given in Eq. (1).

$$s = \alpha t^n, \tag{1}$$

where  $t$  is time,  $\alpha$  and  $n$  are parameters,  $s$  is horizontal axis (Figure 1).

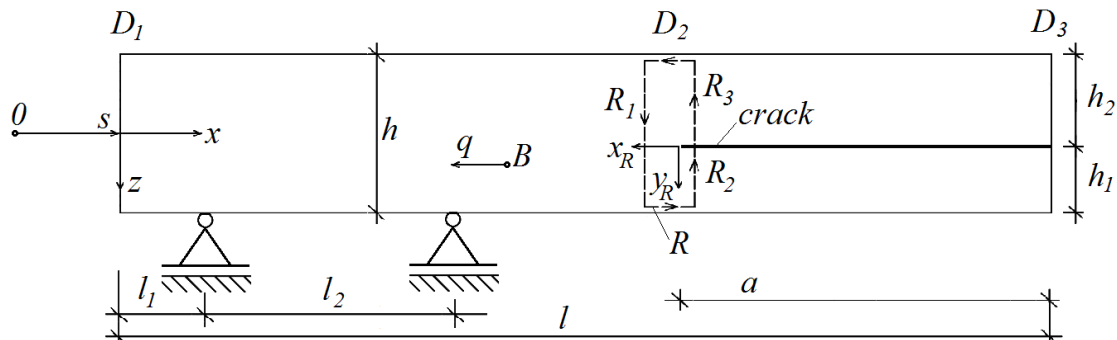


Figure 1. Beam structure with lengthwise crack

The velocity,  $v$ , and the acceleration,  $a$ , of the beam are found by Eqs. (2) and (3), respectively.

$$v = \frac{ds}{dt} = \alpha n t^{n-1}, \tag{2}$$

$$a = \frac{dv}{dt} = \alpha n(n-1)t^{n-2}. \tag{3}$$

The inertia loading,  $q$ , in an arbitrary point,  $B$ , of the beam is obtained by Eq. (4).

$$q = -am, \tag{4}$$

where  $m$  is the mass density. Since the beam is functionally graded along both thickness and length, the mass density varies continuously in transversal and longitudinal direction. The mass density variation in transversal direction is given in Eq. (5).

$$m = m_{\delta} e^{\lambda \frac{h+z}{h}}, \quad (5)$$

where

$$-\frac{h}{2} \leq z \leq \frac{h}{2}. \quad (6)$$

Here,  $m_{\delta}$  is the mass density in the upper surface of the beam,  $\lambda$  is a parameter,  $z$  is the vertical centric axis of the beam,  $h$  is the beam thickness. The quantity,  $m_{\delta}$ , varies along the beam length according to the law given in Eq. (7).

$$m_{\delta} = m_{\delta D1} e^{\mu \frac{x}{l}}, \quad (7)$$

where

$$0 \leq x \leq l. \quad (8)$$

Here,  $m_{\delta D1}$  is the mass density in the left-hand end of the beam,  $\mu$  is a parameter,  $x$  is the longitudinal centroidal axis of the beam,  $l$  is the beam length. Equations (4), (5) and (7) indicate that  $q$  is a continuous function of the time, the transversal and longitudinal coordinates of the beam structure.

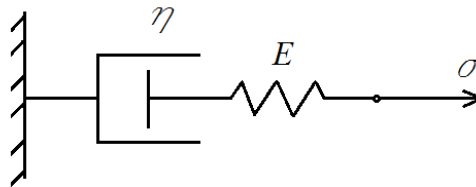


Figure 2. Non-linear viscoelastic model

The beam acted upon by the inertia loading exhibits non-linear viscoelastic behavior. The fully non-linear modification of the classical viscoelastic model of Maxwell depicted in Figure 2 is applied for dealing with the beam structure. Both components, i.e. the spring and the dashpot, of the viscoelastic model in Figure 2 have non-linear behavior that is described by the laws given in Eqs. (9) and (10), respectively.

$$\sigma_E = E \varepsilon_E^{r_E}, \quad (9)$$

$$\sigma_{\eta} = \eta \dot{\varepsilon}_{\eta}^{r_{\eta}}, \quad (10)$$

where  $\sigma_E$  and  $\sigma_{\eta}$  are the stresses in the spring and the dashpot,  $E$ ,  $\eta$ ,  $r_E$  and  $r_{\eta}$  are material parameters,  $\varepsilon_E$  and  $\varepsilon_{\eta}$  are the strains in the spring and the dashpot,  $\dot{\varepsilon}_{\eta}$  is the derivative with respect to time. The model is under stress,  $\sigma$ , that is given in Eq. (11).

$$\sigma = \beta t^{n-2}, \quad (11)$$

where  $\beta$  is a parameter.

It is evident that the stress in both components of the model in Figure 2 are equal to  $\sigma$ , i.e.

$$\sigma_E = \beta t^{n-2}, \quad (12)$$

$$\sigma_{\mu} = \beta t^{n-2}. \quad (13)$$

The strain,  $\varepsilon$ , in the viscoelastic model is found by using Eq. (14).

$$\varepsilon = \varepsilon_E + \varepsilon_\eta. \quad (14)$$

By substituting of Eqs. (12) and (13) in Eqs. (9) and (10), we obtain

$$E\varepsilon_E^{r_E} = \beta t^{n-2}, \quad (15)$$

$$\eta \dot{\varepsilon}_\eta^{r_\eta} = \beta t^{n-2}. \quad (16)$$

From Eqs. (15) and (16), after some mathematical manipuiltions, we derive

$$\varepsilon_E = \left( \frac{\beta t^{n-2}}{E} \right)^{\frac{1}{r_E}}, \quad (17)$$

$$\dot{\varepsilon}_\eta = \left( \frac{\beta t^{n-2}}{\eta} \right)^{\frac{1}{r_\eta}}. \quad (18)$$

By integrating of Eq. (18), we have

$$\varepsilon_\eta = \left( \frac{\beta}{\eta} \right)^{\frac{1}{r_\eta}} \frac{t^{\frac{n-2+r_\eta}{r_\eta}}}{\frac{n-2+r_\eta}{r_\eta}} + C_1. \quad (19)$$

The integration constant,  $C_1$ , is determined by using the initial condition given in Eq. (20).

$$\varepsilon_\eta(0) = 0. \quad (20)$$

From Eqs. (19) and (20), we obtain

$$C_1 = 0. \quad (21)$$

Thus, Eq. (19) is written as

$$\varepsilon_\eta = \left( \frac{\beta}{\eta} \right)^{\frac{1}{r_\eta}} \frac{t^{\frac{n-2+r_\eta}{r_\eta}}}{\frac{n-2+r_\eta}{r_\eta}}. \quad (22)$$

From Eqs. (14), (17) and (21), we obtain the stress-strain-time relation given in Eq. (23).

$$\varepsilon = \left( \frac{\beta t^{n-2}}{E} \right)^{\frac{1}{r_E}} + \left( \frac{\beta}{\eta} \right)^{\frac{1}{r_\eta}} \frac{t^{\frac{n-2+r_\eta}{r_\eta}}}{\frac{n-2+r_\eta}{r_\eta}}. \quad (23)$$

From Eq. (11), we have

$$\beta = \frac{\sigma}{t^{n-2}}. \quad (24)$$

Finally, Eq. (24) is substituted in Eq. (23), i.e.

$$\varepsilon = \left( \frac{\sigma}{E} \right)^{\frac{1}{r_E}} + \left( \frac{\sigma}{\eta} \right)^{\frac{1}{r_\eta}} \frac{r_\eta t}{n-2+r_\eta}. \quad (25)$$

Equation (25) is applied for describing the non-linear viscoelastic behavior of the beam when analyzing the lengthwise fracture under the inertia loading. Since the beam is functionally graded along the thickness and length the material properties,  $E$ ,  $\eta$ ,  $r_E$  and  $r_\eta$ , change continuously in both transversal and longitudinal directions. The following expressions describe this change.

$$E = E_\delta e^{\lambda_E \frac{\frac{h}{2}+z}{h}}, \quad (26)$$

$$\eta = \eta_\delta e^{\lambda_\eta \frac{\frac{h}{2}+z}{h}}, \quad (27)$$

$$r_E = r_{E\delta} e^{\lambda_{rE} \frac{\frac{h}{2}+z}{h}}, \quad (28)$$

$$r_\eta = r_{\eta\delta} e^{\lambda_{r\eta} \frac{\frac{h}{2}+z}{h}}, \quad (29)$$

$$E_\delta = E_{\delta D1} e^{\mu_E \frac{x}{l}}, \quad (30)$$

$$\eta_\delta = \eta_{\delta D1} e^{\mu_\eta \frac{x}{l}}, \quad (31)$$

$$r_{E\delta} = r_{E\delta D1} e^{\mu_{rE} \frac{x}{l}}, \quad (32)$$

$$r_{\eta\delta} = r_{\eta\delta D1} e^{\mu_{r\eta} \frac{x}{l}}, \quad (33)$$

where  $E_\delta$ ,  $\eta_\delta$ ,  $r_{E\delta}$  and  $r_{\eta\delta}$  are the values of  $E$ ,  $\eta$ ,  $r_E$  and  $r_\eta$  in the upper surface of the beam,  $E_{\delta D1}$ ,  $\eta_{\delta D1}$ ,  $r_{E\delta D1}$  and  $r_{\eta\delta D1}$  are the values of  $E_\delta$ ,  $\eta_\delta$ ,  $r_{E\delta}$  and  $r_{\eta\delta}$  are in the left-hand end of the beam,  $\lambda_E$ ,  $\lambda_\eta$ ,  $\lambda_{rE}$ ,  $\lambda_{r\eta}$ ,  $\mu_E$ ,  $\mu_\eta$ ,  $\mu_{rE}$  and  $\mu_{r\eta}$  are material parameters.

As shown in Figure 1, the beam hosts a lengthwise crack of length,  $a$ . The thicknesses of the crack arms are  $h_1$  and  $h_2$  (Figure 1). The lengthwise fracture is studied by the  $J$  integral (Broek, 1986). The following expression is obtained:

$$J = J_{R1} + J_{R2} + J_{R3}, \quad (34)$$

where

$$J_{R1} = \int \left[ u_{01} \cos \alpha_1 - \left( p_{x1} \frac{\partial u_1}{\partial x_R} + p_{y1} \frac{\partial v_1}{\partial x_R} \right) \right] ds_{ct}, \quad (35)$$

$$J_{R2} = \int \left[ u_{02} \cos \alpha_2 - \left( p_{x2} \frac{\partial u_2}{\partial x_R} + p_{y2} \frac{\partial v_2}{\partial x_R} \right) \right] ds_{ct}, \quad (36)$$

$$J_{R3} = \int \left[ u_{03} \cos \alpha_3 - \left( p_{x3} \frac{\partial u_3}{\partial x_R} + p_{y3} \frac{\partial v_3}{\partial x_R} \right) \right] ds_{ct}. \quad (37)$$

Here,  $u_{01}$ ,  $u_{02}$  and  $u_{03}$  are the specific strain energies in sectors,  $R_1$ ,  $R_2$  and  $R_3$ , of the contour of integration,  $R$ . The latter is depicted in Figure 1.  $\alpha_1$ ,  $\alpha_2$  and  $\alpha_3$  are the angles between the outward normal vector and the contour of integration in sectors,  $R_1$ ,  $R_2$  and  $R_3$ , the quantities,  $u_1$ ,  $u_2$  and  $u_3$ , are the horizontal displacements in the corresponding sectors of the counter,  $v_1$ ,  $v_2$  and  $v_3$  are the vertical displacements,  $p_{x1}$ ,  $p_{x2}$  and  $p_{x3}$  are the components of the stress along the horizontal axis in the

corresponding sectors of the contour,  $p_{y1}$ ,  $p_{y2}$  and  $p_{y3}$  are the components of the stress along the vertical axis,  $ds_{ct}$  is an elementary portion of the contour of integration.

The specific strain energy,  $u_{01}$ , involved in Eq. (34) is derived by Eq. (38).

$$u_{01} = \int \sigma d\varepsilon . \quad (38)$$

The strain,  $\varepsilon$ , varies along the beam thickness according to Eq. (39).

$$\varepsilon = \kappa_1(z - z_n), \quad (39)$$

where

$$-\frac{h}{2} \leq z \leq \frac{h}{2}. \quad (40)$$

Here,  $\kappa_1$  and  $z_n$  are the curvature and the neutral axis coordinate, respectively. They are determined from Eqs. (41) and (41).

$$N_1 = \iint_{(A)} \sigma dA, \quad (41)$$

$$M_1 = \iint_{(A)} \sigma z dA, \quad (42)$$

where  $N_1$  and  $M_1$  are the axial force and the bending moment induced by the inertia loading,  $A$  is the area of the cross-section. The other quantities involved in Eq. (35) are obtained as given below.

$$\cos \alpha_1 = 1, \quad (43)$$

$$p_{x1} = \sigma, \quad (44)$$

$$\frac{\partial u_1}{\partial x_R} = \varepsilon, \quad (45)$$

$$p_{y1} = 0, \quad (46)$$

$$ds_{ct} = dz. \quad (47)$$

The axes,  $x_R$  and  $y_R$ , are depicted in Figure 1.

The quantities involved in Eqs. (36) and (37) are derived in a similar way. The integrals in Eqs. (35), (36) and (37) are solved by the MatLab. The integral  $J$  is found by Eq. (34). The lengthwise fracture in the beam under inertia loading is studied also by determining the strain energy release rate,  $G$ , through Eq. (48) for check-up of the  $J$  integral analysis.

$$G = \frac{dU^*}{bda}, \quad (48)$$

where  $U^*$  is the beam complementary strain energy,  $b$  is the beam width.  $U^*$  is found by Eq. (49).

$$U^* = \iiint_{(V)} u_0^* dV, \quad (49)$$

where  $u_0^*$  is the specific complementary strain energy,  $V$  is the beam volume. The strain energy release rate agrees very well with  $J$ -integral which is a check-up of the analysis.

### Parametric Exploration Results

First, by using the integral  $J$  we explore how the lengthwise fracture in the functionally graded viscoelastic beam under inertia loading is influenced by the variable mass density. It is assumed that  $a = 0.200$  m,  $b = 0.015$  m,  $h = 0.022$  m,  $h_1 = 0.011$  m,  $h_2 = 0.011$  m,  $l = 0.900$  m,  $\alpha = 0.3$  and  $\beta = 2.5$ .

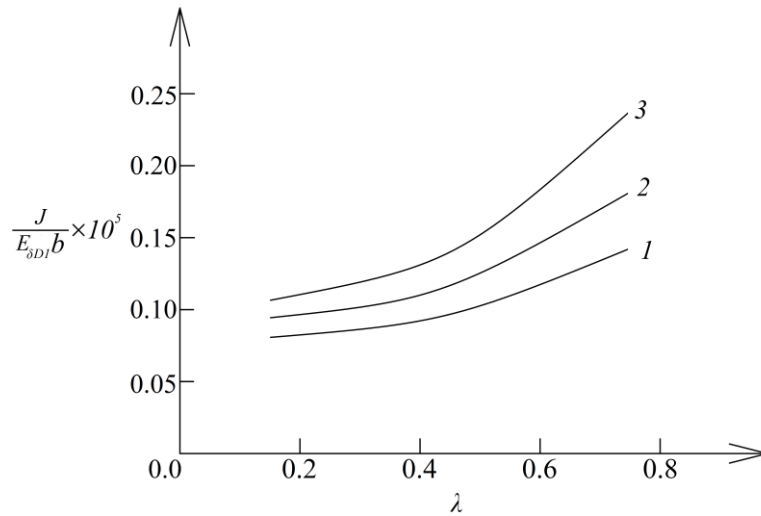


Figure 3. Variation of the integral  $J$  with  $\lambda$

The curves plotted in Figure 3 reveal the change of the integral  $J$  in non-dimensional form induced by change of parameter,  $\lambda$ , at  $\mu = 0.3$  (curve 1),  $\mu = 0.6$  (curve 2) and  $\mu = 0.9$  (curve 3). As already mentioned, the parameters,  $\lambda$  and  $\mu$ , govern the variation of the mass density along the thickness and length of the beam structure depicted in Figure 1. By inspecting the curves in Figure 3, we can conclude that growth of the values of  $\lambda$  and  $\mu$  leads to substantial rise of the integral  $J$ .

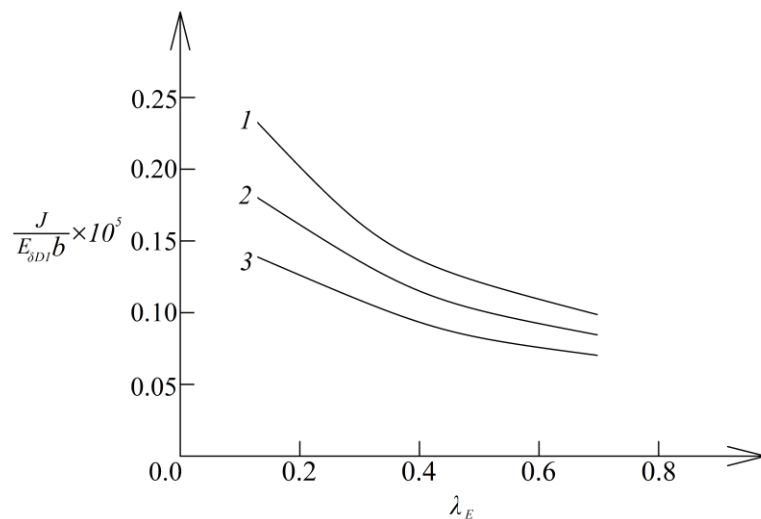


Figure 4. Variation of the integral  $J$  with  $\lambda_E$

Further, it is explored how the lengthwise fracture in the beam is influenced by the variation of parameter,  $\lambda_E$ , at  $\mu_E = 0.2$  (curve 1),  $\mu_E = 0.5$  (curve 2) and  $\mu_E = 0.8$  (curve 3). In this relation, the change of the integral  $J$  in non-dimensional form is depicted in Figure 4. The curves indicate a significant influence of both  $\lambda_E$  and  $\mu_E$  on the lengthwise fracture in the beam (Figure 4). Increase of  $\lambda_E$  and  $\mu_E$  reduces the integral  $J$  as can be observed in Figure 4.

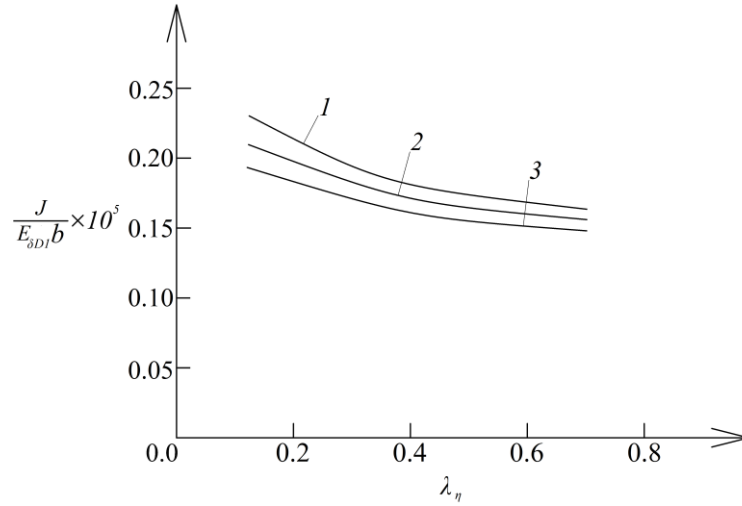


Figure 5. Variation of the integral  $J$  with  $\lambda_\eta$

The influence of parameters,  $\lambda_\eta$  and  $\mu_\eta$ , on the lengthwise fracture is explored too. The corresponding curves are depicted in Figure 5 (curve 1 is for  $\mu_\eta = 0.3$ , curve 2 is for  $\mu_\eta = 0.5$  and curve 3 is for  $\mu_\eta = 0.8$ ). Since  $\lambda_\eta$  and  $\mu_\eta$  are connected to variation of  $\eta$ , the curves in Figure 5 in fact reveal how by varying of  $\eta$  we may influence the lengthwise fracture in the beam. It can be seen in Figure 5 that the growth of  $\lambda_\eta$  and  $\mu_\eta$  has a positive effect on the lengthwise fracture since the integral  $J$  reduces.

## Conclusion

Lengthwise fracture in a functionally graded non-linear viscoelastic beam structure moving in horizontal direction is studied. The attention is focused on the problem of the influence of variation of the mass density on the lengthwise fracture (the mass density varies continuously along both thickness and length of the beam). The other material parameters of the beam also vary continuously. The beam with lengthwise crack is acted upon by inertial load. The integral  $J$  is solved. The analysis performed indicates that the lengthwise fracture is influenced substantially by the variation of the mass density. In particular, the growth of parameters,  $\lambda$  and  $\mu$ , which govern the mass density variation in the beam structure leads to significant growth of the integral  $J$ . It is explored also how the lengthwise fracture is affected by parameters,  $\lambda_E$ ,  $\mu_E$ ,  $\lambda_\eta$  and  $\mu_\eta$  (these parameters govern variation of  $E$  and  $\eta$ ). Growth of  $\lambda_E$ ,  $\mu_E$ ,  $\lambda_\eta$  and  $\mu_\eta$  influences positively the lengthwise fracture since it reduces the integral  $J$ .

## Recommendations

The continuous variation of mass density has to be taken into account in lengthwise fracture analyses of moving functionally graded beam structures.

## Scientific Ethics Declaration

\* The author declares that the scientific ethical and legal responsibility of this article published in EPSTEM journal belongs to the author.

## Conflict of Interest

\* The author declares there is no conflict of interest.

## Funding

\* Not applicable.

## Acknowledgements or Notes

\* This article was presented as an oral presentation at the International Conference on Technology, Engineering and Science ( [www.icontes.net](http://www.icontes.net) ) held in Antalya/Türkiye on November 12-15, 2025.

## References

- Broek, D. (1986). *Elementary engineering fracture mechanics*. Springer.
- Dolgov, M. A. (2024). Analysis of the stress state in the deformed coating under base stretching with the bending effect account. *Strength of Materials*, 56, 1127-1135.
- Fanani, E. W. A., Surojo, E., Prabowo, A. R., & Akbar, H. I. (2021). Recent progress in hybrid aluminum composite: Manufacturing and application. *Metals*, 11, 1919-1929.
- Gandra, J., Miranda, R., Vilaça, P., Velhinho, A., & Teixeira, J. P. (2011). Functionally graded materials produced by friction stir processing. *Journal of Materials Processing Technology*, 211, 1659-1668.
- Hedia, H. S., Aldousari, S. M., Abdellatif, A. K., & Fouda, N. A. (2014). New design of cemented stem using functionally graded materials (FGM). *Biomedical Materials and Engineering*, 24, 1575-1588.
- Mahamood, R. C., & Akinlabi, E. T. (2017). *Functionally graded materials*. Springer.
- Radhika, N., Sasikumar, J., Sylesh, J. L., & Kishore, R. (2020). Dry reciprocating wear and frictional behaviour of B4C reinforced functionally graded and homogenous aluminium matrix composites. *Journal of Materials Research and Technology*, 9, 1578-1592.
- Rizov, V. I. (2024). The effect of delamination between layers in U-shaped members made of functionally graded multilayered viscoelastic materials. *Journal of Applied and Computational Mechanics*, 10, 830-841.
- Rizov, V. I., & Altenbach, H. (2019). On the analysis of lengthwise fracture of functionally graded round bars. *Structural Integrity and Life*, 19, 102-108.
- Shrikantha Rao, S., & Gangadharan, K. V. (2014). Functionally graded composite materials: An overview. *Procedia Materials Science*, 5, 1291-1299.
- Wu, X. L., Jiang, P., Chen, L., Zhang, J. F., Yuan, F. P., & Zhu, Y. T. (2014). Synergetic strengthening by gradient structure. *Materials Research Letters*, 2, 185-191.

---

## Author(s) Information

---

### Victor Rizov

University of Architecture, Civil Engineering and Geodesy  
1 Chr. Smirnensky Blvd. 1046 – Sofia, Bulgaria  
Contact e-mail: [V.RIZOV.FHE@UACG.BG](mailto:V.RIZOV.FHE@UACG.BG)

---

### To cite this article:

Rizov, V. (2025). Effect of variable mass density on lengthwise fracture in functionally graded beams moving in horizontal direction. *The Eurasia Proceedings of Science, Technology, Engineering and Mathematics (EPSTEM)*, 38, 807-815.